STUDY ON A CONSEQUENCE-INFORMED DECISION MAKING FOR EMERGENCY PLANNING ZONE DISTANCE WITH DOSE VERSUS DISTANCE CURVE

Kodai Wadayama[1,2], Retsu Kojo[3], Takafumi Narukawa[4], Takashi Takata[5]

[1] *Nuclear Regulation Authority: 1-9-9, Roppongi, Minato-ku, Tokyo，106-8450, wadayama_kodai_pt7@nra.go.jp*
[2] *The University of Tokyo: 7-3-1 Hongo, Bunkyo-ku, Tokyo, 113-8656, wadayama@nse.t.u-tokyo.ac.jp*
[3] *Nuclear Regulation Authority: 1-9-9, Roppongi, Minato-ku, Tokyo, 106-8450, kojo_retsu_px2@nra.go.jp*
[4] *The University of Tokyo: 7-3-1 Hongo, Bunkyo-ku, Tokyo, 113-8656, narukawa@n.t.u-tokyo.ac.jp*
[5] *The University of Tokyo: 7-3-1 Hongo, Bunkyo-ku, Tokyo, 113-8656, takata_t@n.t.u-tokyo.ac.jp*

ABSTRACT

Emergency preparedness relies heavily on establishing an Emergency Planning Zone (EPZ) to ensure that protective actions are taken for residents based on risk assessments. A critical aspect of this process is to understand the shape of the dose versus distance (D–D) curve. NUREG-0396 proposes that the dose decreases with downwind distance (r) according to a relationship of 1/r–1/r², however, the D–D curve has only been analyzed for containment-intact accidents. In addition, our recent study highlighted differences in the D–D curve under rainy conditions between scenarios involving filtered containment venting system (FCVS) and aerosol-rich scenarios although that analysis was limited to a specific stability class. This study aims to comprehensively evaluate the D–D curve characteristics specifically for aerosol emissions across a wide range of meteorological conditions. Although the 1/r-1/r² rule can be applied under various weather conditions in FCVS scenarios, applying the formula under certain rainy conditions in containment failure scenarios proves difficult. The D–D curve offers critical insights into dose distribution as a function of distance, directly informing the scaling of EPZ boundaries. By linking the shape of these curves to the thermal power of the plant, this methodology can aid in the decision-making process in adjusting EPZ for reactors with varying thermal powers, while ensuring consistent radiological consequences. Future research will focus on developing a revised formulation of the D–D curve, incorporating analysis in the angular (r–θ) direction.

Keywords: dose versus distance (D–D) curve, emergency planning zone, aerosol, stability class, accident scenario

I. INTRODUCTION

Establishing protective action plans for potential nuclear disasters, such as the Fukushima Daiichi Nuclear Power Plant accident, is crucial. A designated area around a commercial nuclear facility that aids offsite emergency planning, such as evacuation and shelter-in-place, is known as the emergency planning zone (EPZ). The emergence of new reactor types, including Small Modular Reactors (SMRs), has sparked discussions about risk-informed methodologies for defining EPZs [1].

The dose versus distance curve (D–D curve) provides essential insights when defining EPZ. Typically, the atmospheric dispersion increases both vertically and horizontally in the wind direction, whereas the concentration of nuclides diminishes as the distance from the release point increases. In addition, the concentration of nuclides in the plume is affected by radioactive deposition and the decay of nuclides during atmospheric dispersion. Consequently, the D–D curve illustrates the typical reduction in dose as the distance from the release point increases. Understanding the shape of this curve is critical for defining the EPZ, specifically the fraction by which the dose decreases when the distance increases by a factor of r [1][2].

NUREG-0396 discusses the shape of the D–D curve [3]. It suggests that dose decreases with distance according to 1/r and 1/r² curves. However, this research was conducted many years ago and focused only on containment-intact accidents, leaving a gap in the analysis of the D–D curve across diverse accident scenarios. Notably, insufficient analyses have been conducted of accident scenarios involving the filtered containment venting system (FCVS), which was implemented after the Fukushima Daiichi accident in Japan.

To address this gap, the authors have previously performed a detailed analysis of D–D curves, including accident scenarios involving an FCVS [4]. The study has revealed that under no rain conditions, the effects of various accident scenarios are minimal. By contrast, rainy conditions demonstrated a significant difference in D–D curves between scenarios with FCVS and

those with containment failure. However, this analysis was restricted to specific atmospheric stability (D stability) and wind speed (1.8 m/s).

Therefore, the objective of this study is to investigate the differences in D–D curves across various accident scenarios, including those utilizing FCVS, and to clarify the characteristics of the D–D curve through a comprehensive assessment under a wide range of meteorological conditions, with a focus on the aerosol fraction in the source term of each accident scenario.

II. MATERIALS AND METHODS

II.A. Calculation of the Amount of Fission Product Released to the Environment and Selection of Accident Scenarios

The amount of **f**ission **p**roduct (FP) released into the environment was calculated by multiplying the initial core inventory of FP by the core release fraction (CRF) for the transition from the core to the containment vessel, the reduction factor (RDF) due to mitigation effects; and the leakage rate from containment to the environment (EF), as shown in Equation (1) [4][5]. The release duration was set to 1 h for all accident scenarios considered, assuming a large boiling water reactor (BWR) with a thermal power of 3,000 MWth.

$$Q_i = Q_i^{INV} F_i^{CRF} (\prod F_{m,i}^{RDF}) F^{EF} \quad (1)$$

where Q_i is release rate of nuclide i to the environment per hour [Bq/h], Q_i^{INV} is initial core inventory of nuclide i (3,000 MWth reactor in WASH-1400 [6]) [Bq], F_i^{CRF} is core release fraction released from the core to the containment vessel (CRF) [-], $F_{m,i}^{RDF}$ is reduction factor of nuclide i by mitigation effect m (RDF) [-], F^{EF} is leakage rate from containment to the environment per hour (EF) [1/h]. The value of CRF was taken from Early in vessel release phase in NUREG-1465 [7]. The chemical form of iodine entering containment was assumed to be composed of 95% aerosol, 4.85% elemental iodine and 0.15% organic iodine [7]. The RDF was defined for each accident scenario, while the EF was set to 1.0, assuming all nuclides in the containment atmosphere are released within one hour duration, because this research focused on the short release.

Table 1 outlines the accident scenarios and the fractions of each nuclide released into the environment, relative to the initial inventory, using Equation (1).

TABLE 1. Accident Scenarios and Environmental Release Fractions of Nuclides

Accident scenario (details are provided in the previous report [4].)	Description of accident scenario	Total release fraction to the environment compared to the initial inventory of each nuclide [-]			
		gas	gas & aerosol	aerosol	
		Xe	I	Cs	Te
CF-6h (small mitigation)	Core melt and release of FP to the environment 6 h after reactor shutdown due to containment failure	9.5E−01	9.0E−02	7.2E−02	1.8E−02
CF-24h (small mitigation)	Core melt and release of FP to the environment 24 h after reactor shutdown due to containment failure	9.5E−01	7.9E−03	6.0E−03	1.5E−03
HV-6h (mid mitigation)	Core melt and release of FP to the environment 6 h after reactor shutdown due to hardened containment venting	9.5E−01	4.9E−03	3.6E−03	9.0E−04
HV-24h (mid mitigation)	Core melt and release of FP to the environment 24 h after reactor shutdown due to hardened containment venting	9.5E−01	7.5E−04	3.0E−04	7.5E−05
FV-6h (large mitigation)	Core melt and release of FP to the environment 6 h after reactor shutdown due to FCVS	9.5E−01	1.4E−05	3.6E−06	9.0E−07
FV-24h (large mitigation)	Core melt and release of FP to the environment 24 h after reactor shutdown due to FCVS	9.5E−01	8.0E−06	3.0E−07	7.5E−08

Noble gases are not subject to mitigation effects and are released in significant quantities in all accident scenarios considered in this study. By contrast, the behavior of aerosol nuclides within the containment depends on the effectiveness of mitigations, so the nuclides which ultimately released to the environment vary in each accident scenario. The mitigation effects considered in this study are containment holdup, scrubbing, and FCVS. The RDFs were assigned based on methods described in previous studies [4]; and their combination defines the overall aerosol removal efficiency. Two holdup durations were assumed to be short-term and long-term, corresponding to environmental release times of 6 and 24 h, respectively. CF-6h and CF-24h are containment failure scenarios in which limited mitigation effect is expected, and a large amount of aerosol radionuclides are released. HV-6h and HV-24h are scenarios using hardened containment venting, which are expected to remove aerosol nuclides moderately due to pool scrubbing effects in addition to holdup. FV-6h and FV-24h are scenarios using FCVS, and most aerosol nuclides are removed due to the strong mitigation effects of holdup, pool scrubbing, and FCVS.

II.B. Calculation Methods for Atmospheric Dispersion, Deposition, and Effective Dose

II.B.1. Calculation of Atmospheric Dispersion and Deposition

The assumed meteorological conditions are described in Table 2. This study considers various atmospheric stability classes and wind speeds, expanding upon the previous report that considered only stability class D and a wind speed of 1.8 m/s. This allows for the calculation of D–D curves under diverse meteorological conditions. We focused on analyzing newly considered effects of atmospheric stabilities and wind speeds, setting the representative precipitation rate at 3.8 mm/h [4] [8]. According to meteorological guidance [9] and Turner's method [10], B and F stabilities are most frequently observed under low-wind conditions. Thus, we assigned a wind speed of 1 m/s to stability classes B and F, and 2–5 m/s to stability class D.

TABLE 2. Meteorological Conditions Considered in the Study

	Stability class	Wind speed [m/s]	Precipitation rate [mm/h]
Past research	D	1.8	0.5, 3.8, 10
This research	B, D, F	1.0–5.0	3.8

Atmospheric dispersion was calculated using the Gaussian plume model, as given in Equation (2). Radioactive material was assumed to be released continuously from the emission source, maintaining a constant wind direction and speed. The diffusion parameters σ_y and σ_z are functions of the distance from the release point and were calculated using the referenced Japanese Meteorological Guidance [9]. The air concentrations of nuclides were computed, as expressed in Equation (3), considering radioactive decay and depletion through dry and wet deposition during atmospheric dispersion. Washout effects due to wet deposition were considered as exponential term in Equation (3) with reference to NUREG-1940 [8].

$$\chi / Q = \frac{1}{2\pi\sigma_y\sigma_z u}\exp\left(-\frac{y^2}{2\sigma_y^2}\right)\left\{\exp\left(-\frac{(z-h)^2}{2\sigma_z^2}\right)+\exp\left(-\frac{(z+h)^2}{2\sigma_z^2}\right)\right\} \tag{2}$$

$$\chi_i(x,y,z) = Q_i\left(\chi / Q\right)\exp\left(-\lambda_i\frac{x}{u}\right)\exp\left(-\Lambda\frac{x}{u}\right)f_F \tag{3}$$

Also, dry deposition velocities were assumed to vary based on atmospheric stability, whereas the particle size distribution was considered constant across all accident scenarios [8]. The depletion factor f_F denotes the reduction in plume concentration caused by dry deposition [11]. In the previous study, only atmospheric stability D was analyzed, and the new depletion factor f_F by dry deposition was not included as it was considered to have little influence [4]. In this study, f_F was newly considered.

$$\chi^{\bullet}_{i,D}(x,y) = \chi_i(x,y,0)\left(V_d + V_R\right) \tag{4}$$

$$V_R = \Lambda\sqrt{\frac{\pi}{2}}\sigma_z\exp\left(\frac{h^2}{2\sigma_z^2}\right) \tag{5}$$

$$f_F = \exp\left[-\sqrt{\frac{2}{\pi}} \frac{V_d}{u} \int_0^x \frac{1}{\sigma_z\left(x'\right)} \exp\left\{ -\frac{h^2}{2\sigma_z^2\left(x'\right)} \right\} dx' \right] \quad (6)$$

where $\chi^{\bullet}_{i,D}$ is nuclide i deposited per unit surface area per unit time [Bq/sm^3], χ_i is air concentration of nuclide i [Bq/m^3], Q_i : Release rate of nuclide i to the environment [Bq/s], u is wind speed [m/s], σ_y is diffusion parameter in the downwind horizontal axis (y axis) [m], σ_z is diffusion parameter in the downwind horizontal axis (z axis) [m], h is release height [m], Λ is washout coefficient [1/s], λ_i is decay coefficient [1/s], V_d is dry deposition velocity [m/s], and V_R is wet deposition rate [m/s].

II.B.2. Calculation of Effective Dose

The effective dose $H_S(x)$ was calculated using Equation (7), which multiplies the spatial concentration and ground surface concentration of radioactivity derived from atmospheric diffusion and deposition, by the dose conversion factor. The details of the calculation are based on previously reported methods considering three exposure pathways. The effective dose was computed by summing 1 hour of cloudshine, 1 hour of inhalation, and 7 days of groundshine, in accordance with IAEA GSR Part 7 [12].

$$H_s(x) = \sum_i K_i^{CS} \chi_i + \sum_i K_i^{GS} \chi^{\bullet}_{i,D} + \sum_i K_i^{IH} \chi_i \quad (7)$$

where $H_s\left(x\right)$ is effective dose for accident scenario *s* at downwind distance x [Sv], K_i^{CS} is dose conversion factor from air concentration to cloudshine dose [Svm^3 / Bq] [13], K_i^{GS} is dose conversion factor from ground deposition to groundshine dose [Svm^2 s/ Bq] [13], K_i^{IH} is dose conversion factor from air concentration to inhalation dose [Svm^3 / Bq] **Error! Reference source not found.**.

II.C. Calculation of the D–D Curve

The ratio $f_s^{DIST}(x)$ (D–D ratio), defined as the "effective dose at 1 km from the release point" relative to the "effective dose at any distance," was calculated for each accident scenario as shown in Equation (8). The corresponding D–D curve was then evaluated. This approach enables a quantitative assessment of the effects of various accident scenarios and meteorological conditions on $f_S^{DIST}(x)$ (D–D ratio) and comparison with the 1/r and 1/r² curves in NUREG-0396.

$$f_s^{DIST}(x) = \frac{H_s\left(x\right)}{H_{s,0}} \quad (8)$$

where $H_s\left(x\right)$ is effective dose for accident scenario *s* at downwind distance x [Sv], and $H_{s,0}$ is effective dose for accident scenario *s* at 1 km [Sv].

III. RESULTS AND DISCUSSION

III.A. Calculation Results of the D–D Curve for the Accident Scenarios without Rainfall

Figure 1 presents the D–D curves for each accident scenario under atmospheric stability D and wind speeds of 2 or 5 m/s. The divergence of the D–D curves among the accident scenarios was minimal, particularly at a wind speed of 5 m/s, suggesting that the D–D curve can generally be approximated by $1/r^{1.5}$ for any accident scenario. This occurs because the effects of phenomena such as radioactive decay of nuclides during atmospheric dispersion and plume depletion through deposition, which primarily drive the divergence in D–D curves, diminish as wind speeds increase.

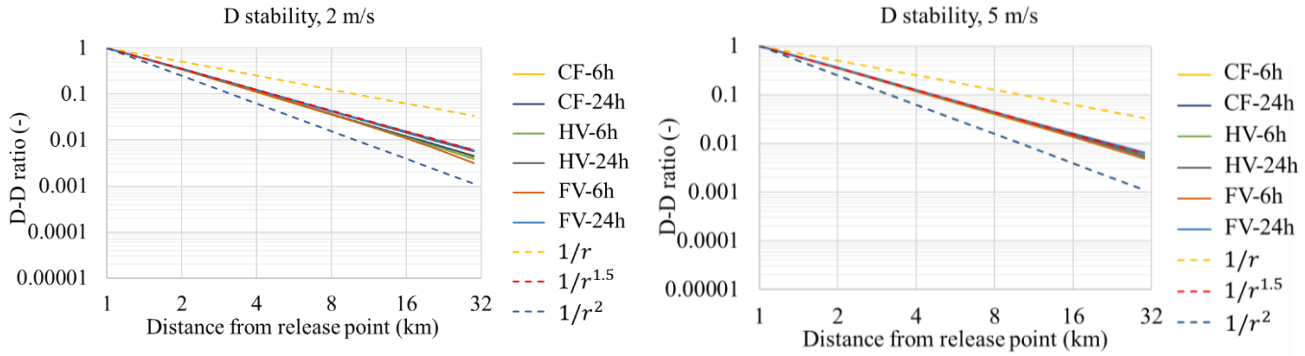

FIGURE 1. D–D Curves of Accident Scenarios under D Stability and Wind Speeds of 2 m/s and 5 m/s (No Rain).

Figure 2 presents the D–D curves for the accident scenarios at atmospheric stabilities B and F with a wind speed of 1 m/s. For atmospheric stability B, the D–D curves exhibited a steep slope, approaching $1/r^2$ at 1–5 km. Beyond approximately 5 km, the plume reached the mixing layer height, halting atmospheric dispersion in the vertical direction (z axis) and allowing horizontal dispersion (y axis) to dominate. As a result, the slopes of the D–D curves were close to $1/r$.

In the case of F stability, although the divergence of the D–D curves among accident scenarios remained small, some differences were noted compared to other stability classes. Specifically, the D–D curve for the scenario involving FCVS at 6 h after shutdown (FV-6h), which was influenced significantly by short-lived nuclides, and the scenarios with containment failure (CF-6h, CF-24h), which were affected by reduced plume concentration due to dry deposition, approached the $1/r^{1.5}$ relationship. By contrast, the D–D curves for the other accident scenarios exhibited a slope that fell between $1/r$ and $1/r^{1.5}$.

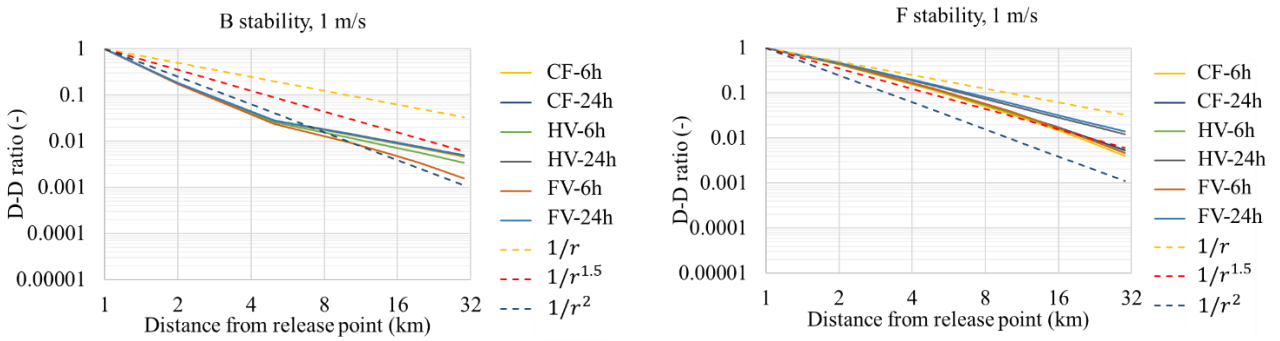

FIGURE 2. D–D Curves of Accident Scenarios under B and F Stabilities and Wind Speeds of 1 m/s (No Rain).

III.B. Calculation Results of the D–D Curve for the Accident Scenarios with Rainfall

Figure 3 presents the D–D curves for the accident scenarios at atmospheric stability D and wind speeds of 2 and 5 m/s. At a wind speed of 2 m/s, the divergence of the D–D curves were pronounced. For containment failure scenarios such as CF-6h and CF-24h, which had a high aerosol contribution, the D–D curves deviated from the NUREG-0396 [3] approximate formula. In these scenarios, the D–D ratios from upwind to downwind were significantly reduced due to aerosol removal by rainfall. By contrast, for accident scenarios utilizing an FCVS, the D–D curves tended to asymptote to $1/r^{1.5}$ in a manner consistent with scenarios without rainfall. However, the D–D curves for the accident scenarios at a wind speed of 5 m/s were less affected by rainfall due to the brief atmospheric dispersion time, resulting in minimal divergence among the D–D curves.

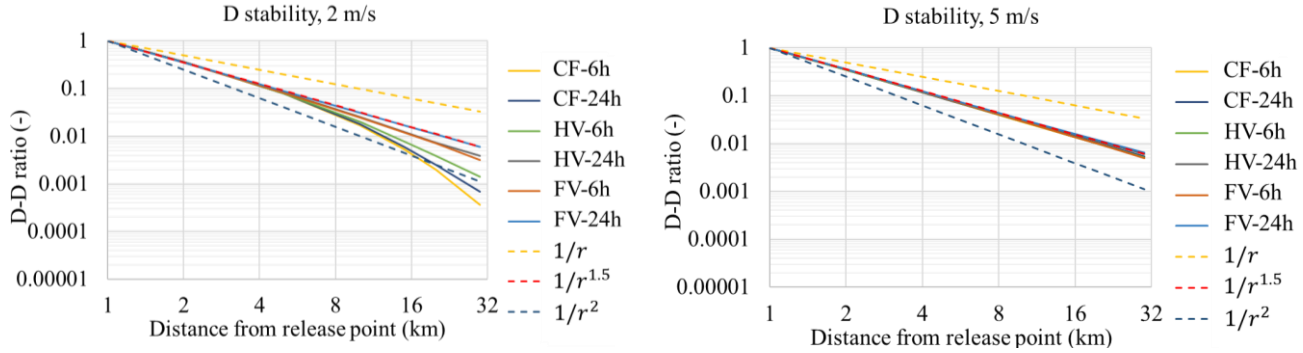

FIGURE 3. D–D Curves of Accident Scenarios under D Stability and Wind Speeds of 2 and 5 m/s (Rain).

Figure 4 presents the D–D curves for the accident scenarios under atmospheric stability conditions B and F at a wind speed of 1 m/s. Similar to the findings under D stability, the D–D curves among different accident scenarios exhibited significant divergence. Specifically, for scenarios with a high aerosol contribution, such as CF-6h and CF-24h (i.e., containment failure scenarios), the results indicated notable discrepancies between the approximate equation of NUREG-0396 [3] and the D–D curves. This suggests that, under rainfall conditions, the NUREG-0396 [3] approximation is challenging to apply to certain accident scenarios.

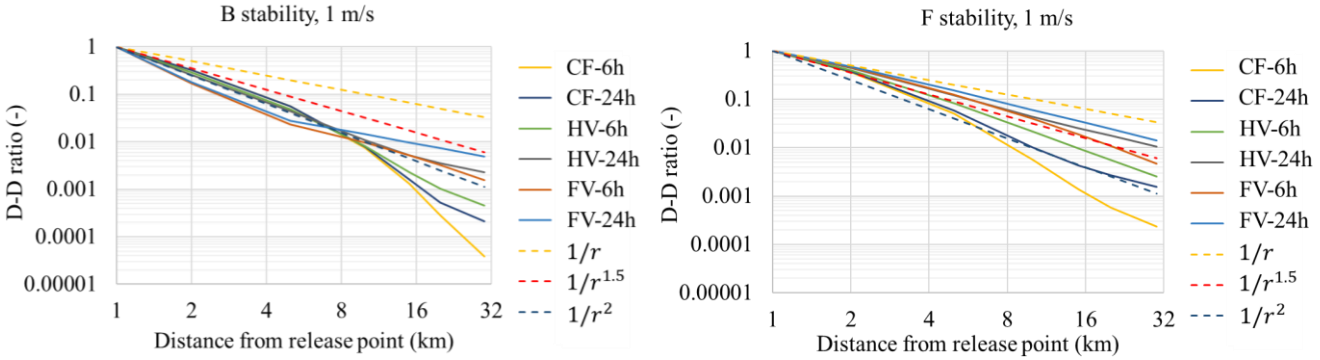

FIGURE 4. D–D Curves of Accident Scenarios under B and F Stabilities and Wind Speeds of 1 m/s (Rain).

III.C. Analysis of Aerosol Nuclides for the Reconstruction of a New D–D Curve Equation

Figure 5 presents the D–D curves for the accident scenarios under atmospheric stability condition F at a wind speed of 1 m/s, assuming that the dose conversion factors for noble gases and organic iodine in Equation (7) were set to zero, thereby focusing solely on aerosol nuclides as contributors to the effective dose. The meteorological conditions analyzed were F stability, with a wind speed of 1 m/s, which showed a marked divergence in the D–D curves among the accident scenarios.

In both cases, regardless of rainfall, minimal divergence was observed in the D–D curves among accident scenarios, suggesting that the D–D curve can be characterized in a way that is independent of the specific accident scenario when considering only aerosol contributions. These findings provide significant insights into the properties of the D–D curve.

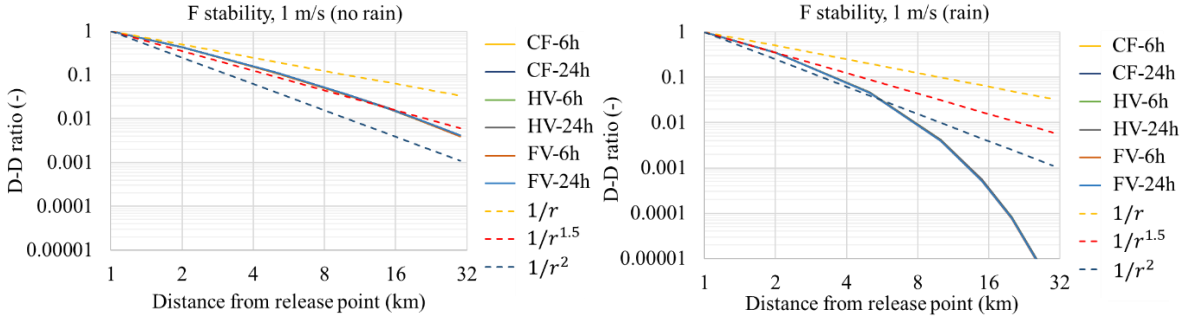

FIGURE 5. D–D Curve for Accident Scenarios Assuming Only the Aerosol Nuclides Contribute to the Dose.

This is attributable to the fact that, when considering only aerosol radionuclide contributions, variations in radionuclide composition among accident scenarios do not significantly affect the deposition of radionuclides on the ground.

We plan to conduct a detailed analysis of this issue and propose a new D–D curve equation to replace the empirical equation presented in NUREG-0396 [3]. However, we should note that the present calculations assumed the dry deposition velocity to be independent of the accident scenario.

IV. APPLICATION OF THIS METHODOLOGY FOR EPZ DETERMINATION: CONSEQUENCE-INFORMED DECISION MAKING

The D–D curve provides critical insights into the dose distribution as a function of distance, facilitating the scaling of EPZ distances based on thermal power [1]. Specifically, under the assumption that thermal power is proportional to the initial core inventory of FP in Equation (1), the proposed methodology utilizing the D–D curve enables the scaling of EPZ for reactors with varying thermal powers, while ensuring consistency in radiological risk.

The establishment of the EPZ is based on the assumption that typical accident conditions, including core damage and containment failure, are consistent regardless of the reactor's thermal power. Equation (9) illustrates the relationship between reactor thermal power and the distance required to reach a dose of 100 mSv, assuming that the D–D ratio is $1/r$. When the thermal power is multiplied by r, the distance to reach 100 mSv is multiplied by r.

$$H_s\left(x_{3000\mathrm{MWth}}\right) = H_s\left(\frac{x_{3000r\mathrm{MWth}}}{r}\right) \tag{9}$$

where $x_{3000MWth}$ is distance to reach 100 mSv in a light water reactor with thermal power of 3,000 MWth [km], and $x_{3000rMWth}$ is distance to reach 100 mSv in a light water reactor with thermal power of 3,000r MWth [km].

For example, compared to a reactor with a thermal power of 3,000 MWth, a reactor with a thermal power of 1,500 MWth would also release only half as much FP into the environment. Figure 6 illustrates the concept of scaling the EPZ based on thermal power by utilizing the D–D curve. By using a $1/r$ D–D curve, we can approximate that the distance required to achieve the dose criteria for defining the EPZ (e.g., 100 mSv effective dose [2] [12]) is 30 km for a reactor with a thermal power of 3,000 MWth, while it is approximately 15 km for a 1,500 MWth reactor, as indicated by (9).

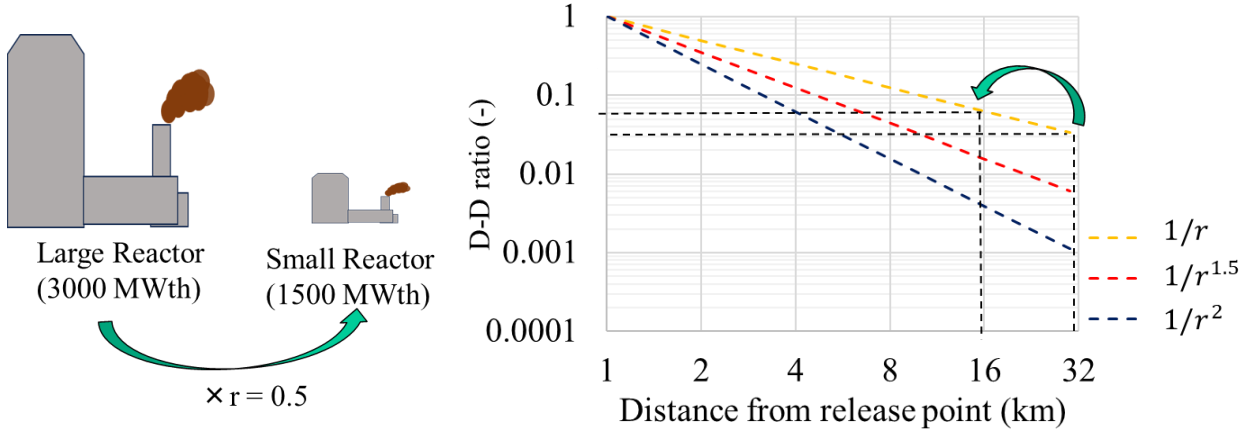

FIGURE 6. Concept of Scaling EPZ Based on Reactor Thermal Power by Utilizing the D–D Curve.

Although this methodology assumes that accident scenarios are similar for both small and large reactors, carefully assessing whether this assumption is valid is crucial [1]. Nonetheless, clarifying the characteristics of the D–D curve is an important initial step toward making consequence-informed decisions, where the EPZ is determined based on equivalent risk considerations for reactors with different thermal powers.

V. CONCLUSIONS

A comprehensive assessment of the characteristics of the D–D curves under a variety of meteorological conditions was performed, where the range of applicability of the $1/r \sim 1/r^2$ D–D curves proposed in NUREG-0396 was quantified. For scenarios involving containment failure without rainfall and significant aerosol contributions, the basic $1/r^{1.5}$ rule was found to be a reliable approximation in most cases, based on the meteorological guidance assumptions. By contrast, under scenarios involving rainfall, the $1/r \sim 1/r^2$ rule could be applied to situations with FCVS. Note that this proved to be challenging in accident scenarios involving containment failure without an FCVS.

The variability of D–D curves across different accident scenarios, including those employing an FCVS, was assessed. The authors' earlier conclusion that "the divergence of D–D curves among accident scenarios is small in the case of no rainfall, but large in the case of rainfall" was confirmed to hold across a wide range of meteorological conditions.

This methodology, leveraging the D–D curve, represents an initial step toward a new consequence-informed decision-making process that aims to establish appropriate EPZ while considering the equivalent risks associated with different reactor thermal power.

This study determined that the D–D curve remains largely independent of accident scenarios when considering only aerosol contributions. A more thorough analysis is expected to yield a more robust approximation that can replace the empirical formula currently proposed in NUREG-0396 [3].

The Gaussian plume model was applied only to the accident scenario involving a 1-h release duration, and the analysis was conducted under conditions of constant wind direction. Future research will expand this approach by incorporating angular (r-θ) directionality and exploring various accident scenarios for emission duration, ultimately enhancing the reliability of the analysis.

REFERENCES

[1] M. Iivonen, "Review of SMR siting and emergency preparedness," Finland: VTT Technical Research Centre of Finland, VTT Research Report No. VTT-R-01612-20 (2022).
[2] IAEA, "Actions to Protect the Public in an Emergency due to Severe Conditions at a Light Water Reactor," Vienna: International Atomic Energy Agency, EPR-NPP-PPA (2013).
[3] U.S. Nuclear Regulatory Commission, "Planning basis for the development of state and local government radiological emergency response plans in support of light water nuclear power plants," NUREG-0396 (1978).
[4] K. Wadayama, R. Kojo, T. Niisoe, "The effect of using Filtered Containment Venting System on variation in dose with distance in the prompt accident consequence assessment," *Journal of Nuclear Science and Technology*, 61:9, 1248–1264 (2024).
[5] T.J. McKenna, J. Trefethen, K. Gant, et al. "Response technical manual: RTM-96," Washington, DC: U.S. Nuclear Regulatory Commission, NUREG/ BR-0150, Volume 1, Revision 4 (1996).
[6] U.S. Nuclear Regulatory Commission, "Reactor safety study: an assessment of accident risks in U.S. Commercial nuclear power plants," WASH-1400 (1975).
[7] L. Soffer, S.B. Burson, C.M. Ferrell, et al. Accident source terms for light-water nuclear power plants. Washington, DC: U.S. Nuclear Regulatory Commission, NUREG-1465 (1995).
[8] J.V. Ramsdell, G.F. Athey, S.A. McGuire, et al. "RASCAL 4: description of models and methods," Washington, DC: U.S. Nuclear Regulatory Commission, NUREG-1940, (2012).
[9] NSC, "Meteorological guidance for reactor safety analysis" [in Japanese], (1982, revised in 2001)
[10] Turner, D. Bruce. "A Diffusion Model for an Urban Area," *Journal of Applied Meteorology and Climatology*, 3:1, 83–91 (1964).
[11] A.J. Nosek, N. Bixler. "MACCS theory manual," Albuquerque: Sandia National Laboratories, SAND2021-11535 (2021).
[12] IAEA, "Preparedness and response for a nuclear or radiological emergency," Vienna: International Atomic Energy Agency, IAEA Safety Standards Series No. GSR Part 7 (2015).
[13] K.F. Eckerman, J.C. Ryman, "External exposure to radionuclides in air, water, and soil," Washington, DC: U.S. Environmental Protection Agency, EPA-402-R-93-081 (1993).
[14] K.F. Eckerman, A.B. Wolbarst, A.C.B. Richardson, "Limiting values of radionuclide intake and air concentration and dose conversion factors for inhalation, submersion, and ingestion," Washington, DC: U.S. Environmental Protection Agency, EPA-520/1-88-020 (1988).